ROS-Induced Nanotherapeutic Approach for Ovarian Cancer Treatment Based on the Combinatorial Effect of Photodynamic Therapy and DJ-1 Gene Suppression

Citation	Schumann, C., Taratula, O., Khalimonchuk, O., Palmer, A. L., Cronk, L.M., Jones, C. V., Escalante, C. A., & Taratula, O. (2015). ROS-Induced Nanotherapeutic Approach for Ovarian Cancer Treatment Based on the Combinatorial Effect of Photodynamic Therapy and DJ-1 Gene Suppression. [Article in Press]. Nanomedicine: Nanotechnology, Biology and Medicine. doi:10.1016/j.nano.2015.07.005
DOI	10.1016/j.nano.2015.07.005
Publisher	Elsevier
Version	Accepted Manuscript
Terms of Use	http://cdss.library.oregonstate.edu/sa-termsofuse

ROS-Induced Nanotherapeutic Approach for Ovarian Cancer Treatment Based on the Combinatorial Effect of Photodynamic Therapy and *DJ-1* Gene Suppression

Canan Schumann, PharmD[a], Olena Taratula, PhD[a], Oleh Khalimonchuk, PhD[b], Amy L. Palmer, MS[c], Lauren M. Cronk[a], Carson V. Jones, BS[a], Cesar A. Escalante, BS[a], Oleh Taratula, PhD[a*]

[a]Department of Pharmaceutical Sciences, College of Pharmacy, Oregon State University, Portland, OR 97201, USA

[b]Department of Biochemistry and Redox Biology Center, University of Nebraska-Lincoln, Lincoln, NE 68588, USA

[c]Department of Veterinary Medicine, College of Veterinary Medicine, Oregon State University, Corvallis, OR 97331, USA

[*]Corresponding author. Tel.: +503-346-4704

E-mail address: Oleh.Taratula@oregonstate.edu

Department of Pharmaceutical Sciences

College of Pharmacy

Collaborative Life Science Building

2730 SW Moody Ave., Mail Code: CL5CP

Portland, OR 97201-5042

The word counts for Abstract: 146 words

Complete manuscript word count: 4,984 words

Number of references: 51

Number of figures: 7

The authors declare no conflicts of interest.

This research was supported by the Medical Research Foundation of Oregon and the College of Pharmacy at Oregon State University. The funding sources had no involvement in the collection, analysis and interpretation of data; and in the decision to submit the article for publication.

Abstract

This study represents a novel approach for intraoperative ovarian cancer treatment based on the combinatorial effect of a targeted photodynamic therapy (PDT) associated with suppression of the DJ-1 protein, one of the key players in the ROS defense of cancer cells. To assess the potential of the developed therapy, dendrimer-based nanoplatforms for cancer-targeted delivery of near-infrared photosensitizer, phthalocyanine, and *DJ-1* siRNA have been constructed. *In vitro* studies revealed that therapeutic efficacy of the combinatorial approach was enhanced when compared to PDT alone and this enhancement was more pronounced in ovarian carcinoma cells, which are characterized by higher basal levels of DJ-1 protein. Moreover, the ovarian cancer tumors exposed to a single dose of combinatorial therapy were completely eradicated from the mice and the treated animals showed no evidence of cancer recurrence. Thus, the developed therapeutic approach can be potentially employed intraoperatively to eradicate unresactable cancer cells.

Key words: ROS, DJ-1, siRNA therapy, photodynamic therapy, ovarian cancer

Abbreviations: PDT - photodynamic therapy; ROS - reactive oxygen species; Nrf2 - nuclear factor (erythroid-derived 2)-like 2; Pc - phthalocyanine; PPIG4 - Generation 4 poly(propylene imine) dendrimer; PPI-siRNA – poly(propylene imine) dendrimer based siRNA delivery system; PPI-Pc – poly(propylene imine) dendrimer based phthalocyanine delivery system; MAL-PEG-NHS - α-Maleimide-ω-N-hydroxysuccinimide ester poly(ethylene glycol), LHRH - Luteinizing Hormone-Releasing Hormone; PY1 - Peroxy Yellow 1; SOGS - Singlet Oxygen Sensor Green; H&E – hematoxylin and eosin; HUVEC - human umbilical vein endothelial cell line; qPCR - real-time quantitative polymerase chain reaction; SD - standard deviation.

Background

Each year there are about 22,000 new cases of ovarian cancer in the US, and more than 14,000 women die from it annually.[1] The high mortality rate is attributed to the fact that 60% of cases are diagnosed at an advanced stage, after the cancer has already metastasized to the abdominal cavity.[2] Currently, surgical resection of the abdominal metastases can significantly reduce ovarian cancer recurrence and, therefore, improve patient survival.[2, 3] Even with the best microsurgical techniques, surgeons leave behind microscopic tumors that eventually lead to cancer relapse.[2, 4, 5] Therefore, there is a critical need for adjuvant intraoperative therapies that can be delivered immediately after tumor resection to kill cancer cells that may be left behind. Intraoperative radiotherapy and hyperthermic chemotherapy showed some potential for sterilization of unresected tumors.[6-8] However, high toxicity and cancer-cell resistance compromise the effectiveness of these modalities.

Unlike radiotherapy or chemotherapy, photodynamic therapy (PDT) is characterized by minimal side effects because it selectively kills cancer cells using a non-toxic photoactive drug (photosensitizer), specifically activated by targeted light.[9] In PDT, cytotoxic reactive oxygen species (ROS) are generated upon light illumination of a specific wavelength by the photosensitizer that has accumulated in the cancer cells.[9, 10] Therefore, PDT offers a higher therapeutic selectivity for cancer cells because of the ability to focus light on cancerous tissue.[10] Moreover, cancer cells have elevated basal ROS levels compared to normal cells, because of their accelerated metabolism and signaling aberrations.[11, 12] Consequently, these malignant cells are selectively vulnerable to further oxidative insults induced by the ROS-generating photosensitizers.[11, 13] The PDT agents, injected prior to surgery accumulate in cancer tumors, and can be activated with the light of a specific wavelength intraoperatively to further enhance surgical outcomes by elevating ROS levels within the cancer tissue, thus causing increased cell

death. The therapeutic potential of intraoperative PDT has already been demonstrated in clinics for treatment of several cancers.[14-16]

Antioxidant defense systems in cancer cells, however, can decrease the efficacy of PDT by scavenging excessively produced ROS.[17] The mechanisms of intracellular antioxidant defense systems involve upregulation of multiple molecules, including superoxide dismutase, Nrf2, glutathione peroxidase and DJ-1, in response to an increase in intracellular ROS levels.[18-21] Among the other proteins, DJ-1 plays a significant role in protecting cancer cells from ROS-mediated apoptosis.[19, 22, 23] DJ-1 increases reduced glutathione synthesis and destabilizes the interaction between Nrf2 and its redox-sensitive cytosolic inhibitor Keap1. Dissociation of the Keap1/Nrf2 complex permits nuclear translocation of Nrf2, which acts as a master transcriptional regulator that induces expression of numerous antioxidant proteins.[19, 22, 23] Moreover, a direct role of DJ-1 in inhibition of the apoptotic pathway has been proposed, based on its ability to reduce the expression of pro-apoptotic protein Bax and inhibit caspase activation.[24] Additionally, overexpression of DJ-1 in various cancer cells is associated with invasion, metastasis, resistance to chemotherapy, and overall cell survival.[19] Based on these facts, we hypothesized that suppression of DJ-1 can enhance the anticancer effect of ROS induced by PDT.

Here, we have developed and evaluated a novel ROS-induced nanotherapeutic approach for intraoperative ovarian cancer treatment based on the combinatorial effect of targeted PDT and suppression of the *DJ-1* gene (Fig. 1). For this modality, we employed two therapeutic agents: (1) phthalocyanine (Pc) as the near infrared (NIR) photosensitizer[25-27] and (2) siRNA as a *DJ-1* gene suppressor. NIR photosensitizers are required for the efficient treatment of deep-seated cancer tumors by PDT, because they can overcome the major obstacles of conventional

photoactive drugs associated with the limited tissue penetration of visible light used for their activation.[10] The employed Pc molecules are characterized by strong absorption of NIR light coupled with efficient ROS-generating properties.[25] To attenuate the intracellular ROS defense system, siRNA therapy gives an opportunity to specifically inhibit the targeted proteins, including DJ-1.[28, 29] However, the stability of siRNA molecules in blood, lack of targeting to the cancer tumors, and limited ability to penetrate across the cellular membrane, have been the major issues in clinical applications.[29] Furthermore, *in vivo* application of Pc is also limited by low water solubility, aggregation and lack of cancer specificity.[25] The development of the nanomedicine platforms for both Pc and *DJ-1* siRNA delivery to ovarian cancer cells and an evaluation of combinatorial ROS-induced therapy both *in vitro* and *in vivo* are reported herein.

Methods

Materials

Human ovarian cancer (A2780/AD and ES2) and human umbilical vein endothelial cell lines (HUVEC) were obtained from ATCC (Manassas, VA). Generation 4 poly(propylene imine) dendrimer (PPIG4) was purchased from SyMO-Chem (Netherlands). α-Maleimide-ω-N-hydroxysuccinimide ester poly(ethylene glycol) (MAL-PEG-NHS, 5 kDa) was acquired from NOF Corporation (White Plains, NY). Luteinizing Hormone-Releasing Hormone (LHRH) peptide (Gln-His-Trp-Ser-Tyr-DLys(DCys)-Leu-Arg-Pro-NH-Et), was obtained from Amersham Peptide Co. (Sunnyvale,CA). siRNA and Singlet Oxygen Sensor Green (SOSG) assay were from Life Technologies (Grand Island, NY). All other chemicals were purchased from VWR.

Synthesis of Pc and DJ-1 *siRNA delivery nanoplatforms*

A Pc-loaded dendrimer nanoplatform functionalized with PEG and LHRH peptide (PPI-Pc) was synthesized according to our previously developed procedure (Supplementary Materials).[26, 27, 30] Synthesis of the *DJ-1* siRNA delivery vehicle (PPI-siRNA) was carried out by first obtaining the PPIG4-siRNA complex via mixing *DJ-1* siRNA (10 μM) and PPIG4 (0.33 μg/ml) in milliQ water. The mixture was incubated at room temperature (RT) for 1 h, followed by the addition of MAL-PEG-NHS (0.033 mg/mL). Next, the LHRH peptide (5 mg/mL) was added to the reaction mixture, followed by shaking overnight at 1300 rpm. The complete complexation of the added siRNA (10 μM) by PPIG4 was validated by the gel retardation assay (Fig. S1). Finally, the PPI-siRNA was purified by dialysis.

Characterization of PPI-Pc and PPI-siRNA nanoplatforms

AFM, zeta potential and hydrodynamic diameter of the prepared complexes were measured as previously described.[26, 31, 32] Flow cytometery was used to evaluate cellular internalization efficiency of both the PPI-Pc and PPI-siRNA.[26, 27] The amount of intracellular singlet oxygen ($^1O_2$) produced by PPI-Pc after light treatment was measured by the SOSG assay.[26] qPCR and Western immunoblotting analysis were employed to measure *DJ-1* gene and protein levels.[32] Additional details can be found in Supplementary Materials.

In vitro *evaluation of ROS-induced combinatorial therapy*

Cells were seeded in a 96-well plate at a density of $1x10^4$ cells/well and treated with the *DJ-1* PPI-siRNA (siRNA=1 μM) 24 h prior to PDT. Afterwards, an additional 100 μL of media containing the various final concentrations of PPI-Pc (0 – 250 ng/mL) was added to an

appropriate well and allowed to incubate for 12 h. After treatment, the cells were rinsed with DPBS three times. Next, PDT was carried out by irradiating the transfected cells with a continuous wave laser diode at 690 nm (Thorlabs Inc, Newton, NJ, 0.3 W/cm^2) for 5 min. All treated samples had proper dark controls for comparison. A modified Calcein AM assay was then used to evaluate cell viability after treatment with the appropriate formulations (Supplementary Materials).[26, 30] Peroxy Yellow 1 (PY1) was employed to quantify the generated intercellular level of H_2O_2 in A2780/AD and ES2 cells after PDT and combinatorial therapy (Supplementary Materials).[33] Analysis of real time A2780/AD cell proliferation after treatment with PPI-siRNA was carried out using the xCELLigence instrument (Supplementary Materials).[34]

In vivo *studies*

Animal studies were performed according to the Humane Care and Use of Laboratory Animals Policy and were approved by Institutional Animal Care and Use Committee of the Oregon State University. Experiments were carried out on nude mice bearing subcutaneous xenografts of A2780/AD cancer cells as previously described (Supplementary Materials).[26, 27, 30] When tumor size became ~ 40 mm^3, the animals were randomly selected to one of seven groups (5 mice per group): (1) control, (2) light, (3) PPI-Pc (Pc dark), (4) PPI-siRNA (DJ-1), (5) PPI-Pc + 690 nm light (PDT), (6) PPI-siRNA + PPI-Pc (DJ-1/Pc dark), and (7) PPI-siRNA + PPI-Pc + 690 nm light (DJ-1/PDT). Mice in groups 6 and 7 underwent intravenous (*i.v.)* injection with the PPI-siRNA (siRNA = 17 μM) followed by injection of PPI-Pc (300 μg/mL) after 24 h. Mice in groups 1, 3, 4 and 5 were injected with saline, PPI-Pc, PPI-siRNA and PPI-Pc, respectively. After 12 h of the last injection, the subcutaneous tumors in the mice from the groups 2, 5, 6 and 7 underwent one-time light treatment (690 nm laser diode, 1.3 W/cm^2, 10 min).[30] The body weight

and tumor size were recorded for all mice during 25 days after treatment. All the tumors were harvested at the end of treatment, processed and used for Hematoxylin and eosin (H&E) counterstaining, Hoechst staining and immunofluorescence chemistry (Supplementary Materials).[32]

Statistical analyses

Data were analyzed using descriptive statistics, single-factor analysis of variance (ANOVA), and presented as mean values ± standard deviation (SD) from three to six independent measurements. The comparison among groups was performed by the independent sample Student's *t*-test. The difference between variants was considered significant if $P < 0.05$.

Results

Preparation and characterization of the nanomedicine platforms for delivery of Pc and siRNA

The structure of PPIG4 dendrimers, having a combination of interior hydrophobic pockets and peripheral hydrophilic primary amines, offer the possibility to encapsulate the hydrophobic Pc molecules, and thereby both decreasing their aggregation while enhancing water solubility[26, 27, 30] (Fig. 1A). Our data indicated that the loading efficiency of Pc into PPIG4 dendrimer is 20% w/w. Furthermore, the positively charged primary amines on the periphery of PPIG4 have been employed for electrostatic complexation of negatively charged siRNA molecules. The dendrimer and siRNA molecules spontaneously self-assemble into nanoparticles. An excess of dendrimers provides encapsulation of siRNA molecules inside of the nanoparticles, which in turn protect the siRNA against serum nuclease degradation and facilitate cellular internalization (Fig. 1B).[36, 37] We have previously demonstrated that the PPIG4 is the most efficient nanoplatform for the

complexation and transfection of siRNA into the cancer cells among other generations of dendrimers.[37]

To enhance stability and biocompatibility of the developed nanoplatforms, the amine-terminated-dendrimer surface has been modified with a PEG, which contains an amine-reactive NHS ester and thiol-reactive maleimide (MAL) group on the opposite ends. The PEGylation has been carried out by coupling NHS groups of PEG to amino groups on the dendrimer surface via amide bonds (Fig. 1A and B).[27, 30, 32] To provide cancer specificity, the nanoplatforms were equipped with a LHRH peptide as a ligand to LHRH receptors that are overexpressed in ovarian cancer cells.[32] The LHRH peptide has been conjugated to the distal end of PEG by coupling the MAL of PEG to cysteine thiol presented in the LHRH sequence (Fig. 1A and B).[27, 32] The average zeta potential values of the LHRH-targeted complexes are +24.4 ± 3.5 mV and +11.9 ± 0.2 mV for PPI-Pc and PPI-siRNA, respectively. The hydrodynamic diameters of the complexes, PPI-Pc and PPI-siRNA, are 62.3 ± 0.1 nm and 147.5 ± 0.2 nm, respectively (Fig. S2A). The larger size of PPI-siRNA in comparison to PPI-Pc is attributed to a fact that several dendrimers and siRNA molecules are incorporated into the final complex as reported previously (Fig. 1B).[37] The AFM images revealed a spherical shape of both nanoplatforms and verified a difference in size between PPI-Pc and PPI-siRNA (Fig. S2B-C). Recorded sizes for both nanoplatforms are within the desired range of 10 − 200 nm to prevent elimination by the kidneys (>10 nm), recognition by macrophage cells (<200 nm), as well as enhancing tumor-targeted delivery via the EPR effect (<200 nm).[39]

The critical feature for these nanoplatforms is the ability to prevent drug leaching in the systemic circulation, thus minimizing side effects. Therefore, the release of hydrophobic Pc from the nanoplatform was assessed in human plasma, which indicated minimal Pc release (less than 2%)

(Fig. S3). The previous studies also suggested that Pc does not have to be released from the dendrimers in the cancer cells to cause the PDT effect.[26, 27, 30, 40] Finally, negligible leaching of siRNA from the nanoplatform in the presence of serum was also confirmed (Fig. S4). Of note, an efficient suppression of DJ-1 mRNA in the cancer cells treated with PPI-siRNA indicates successful release of siRNA in the cytoplasm (Fig. 2).

To evaluate efficiency of the nanoplatforms for delivery of *DJ-1* siRNA and Pc to the ovarian cancer cells, flow cytometry analysis was employed. siRNA was labeled with FITC, while the intrinsic NIR fluorescence of Pc was used to quantify cellular uptake of both nanoplatforms. Flow cytometry analysis showed that the appropriate fluorescence signal was detected in 97.8% and 98.8% ES2 ovarian carcinoma cells after incubation with PPI-Pc (Pc = 63 ng/mL) and PPI-siRNA (siRNA = 1 μM), respectively (Fig. 2A and B). Following a 24 h incubation with the prepared PPI-siRNA (siRNA=1 μM) and washing with DPBS buffer, qPCR analysis revealed downregulation of *DJ-1* mRNA by 90% in ES2 cells as compared to non-treated cells (Fig. 2C). The suppression of the corresponding DJ-1 protein was confirmed via immunoblotting analysis (Fig. 2C inset). The cytotoxic mechanism of Pc toward cancer cells following light activation involves production of ROS mainly in the form of singlet oxygen ($^1O_2$).[10] SOGS assay demonstrated an efficient generation of $^1O_2$ in PPI-Pc-pretreated cells after their exposure to 690 nm light for 5 min (Fig. 2D). This experiment also revealed that the intracellular $^1O_2$ level depends on the Pc concentration. Thus, a 23-fold increase in the intracellular $^1O_2$ level was detected after incubation of ES2 cells with 125 ng/mL of PPI-Pc when compared to PPI-Pc-treated cells under dark conditions. At lower PPI-Pc concentration (32 ng/mL), the $^1O_2$ level was increased only 18 times (Fig. 2D). The non-irradiated cells exhibited negligible increases in singlet oxygen at all PPI-Pc concentrations, confirming that $^1O_2$ is formed

only in the presence of PPI-Pc followed by light irradiation. Thus, the developed PPI-Pc exhibited no dark cytotoxicity at the highest studied concentration of 250 ng/mL (Fig. S5A). In addition, the combination of PPI Pc with the PPI-siRNA nanoplatform loaded with *DJ-1* siRNA (1 μM) did not compromise viability of cancer cells (Fig. S5A).

In vitro *evaluation of ROS-induced combinatorial therapy*

ES2 human clear cell ovarian carcinoma and A2780/AD doxorubicin resistant human ovarian carcinoma cells were used. As shown in Fig. 3A, the basal level of *DJ-1* mRNA in ES2 cells is 1.5 times higher as compared to non-malignant HUVEC cells. In contrast, the A2780/AD cells are characterized by 3.5- and 2.3 fold increases in the intracellular level of *DJ-1* mRNA when compared to HUVEC and ES2 cells, respectively (Fig. 3A). The difference in DJ-1 protein expression in the employed cell lines was further confirmed by immunoblotting (Fig. 3A inset). The selected ovarian cancer cell lines also overexpress LHRH receptors, which assure efficient internalization of the developed LHRH-targeted nanoplatforms.[32, 41, 42]

When ES2 and A2780/AD cells were subjected to PDT via incubation with PPI-Pc nanoplatform for 12 h followed by light irradiation with a 690 nm laser diode for 5 min (0.3 W/cm^2), a distinct cytotoxic effect was detected at all studied concentrations of Pc in both cell lines (Fig. 3B). However, ES2 cells, which exhibited lower DJ-1 protein expression, were more sensitive to PDT. For example, viability of ES2 cells treated with PPI-Pc nanoplatform at the lowest studied concentration of 32 ng/mL was 20% lower when compared to A2780/AD cells. We next examined whether suppression of DJ-1 would enhance the anticancer effect of PDT through the inhibition of cellular antioxidative defense mechanism and, consequently, amplified elevation of intracellular ROS levels. ROS-induced combinatorial therapy was achieved by pre-

treating both ovarian cancer cells 24 h prior to PDT with the siRNA-loaded nanoplatform thereby allowing enough time for intracellular DJ-1 protein degradation and suppression of the cells' antioxidant defense mechanisms. Immunoblotting analysis validated that intracellular level of DJ-1 protein was substantially inhibited in the selected cell lines following 24 h incubation with the PPI-siRNA (Fig. 3C and D, insets). In the next step cells were incubated with PPI-Pc at various concentrations (0 – 250 ng/mL) for 12 h following irradiation with a laser diode for 5 min (0.3 W/cm^2). The recorded data demonstrated that therapeutic efficacy of the combinatorial approach was improved by 6-20% when compared to PDT alone in both cell lines (Fig. 3C and D), and this effect was more pronounced in A2780/AD cells, which are characterized by higher basal level of DJ-1 protein (Fig. 3D). For example, in comparison to PDT alone, the attenuation in viability of the A2780/AD and ES2 cells sequentially treated with PPI-siRNA and PPI-Pc nanoplatform at the concentration of 32 ng/mL was 16% and 6%, respectively. It is noteworthy that combinatorial treatment performed by using the highest concentrations of PPI-siRNA (1μM siRNA) and PPI-Pc (250 Pc ng/mL) demonstrated negligible cytotoxicity toward cancer cells under dark conditions (Fig. S5). When non-treated A2780/AD and ES2 cells or the cells treated with PPI-siRNA only were irradiated with a 690 nm laser diode (0.3 W/cm^2) for 5 min, no decrease in cell viability was recorded (Fig. 3 B-D, controls). It is related to a fact that a 690 nm laser alone at this power density does not increase intracellular ROS level (Fig. 2 D) or generate hyperthermia (Fig. S6).[26]

In addition to regulating oxidative cellular stress, several studies have demonstrated an anti-apoptotic and anti-proliferative functions of DJ-1 through repression of p53 transcriptional activity.[19] Therefore, we also assessed whether treatment of the cancer cells with only *DJ-1* siRNA delivered by PPI-siRNA decreases cell proliferation or induces cellular apoptosis and

contributes to the enhancement of ROS-elevation combinatorial therapy. Our data demonstrated that the viability of both cancer cell lines treated with only the PPI-siRNA nanoplatform was not significantly compromised within 48 h, a period of time required to complete the combinatorial therapy (Fig. 4A). Real-time proliferation studies further confirmed that *DJ-1* siRNA alone does not influence ovarian cancer cells proliferation within 48 h. Cell proliferation started to continuously decrease only after 50 h as compared to the cells treated with the same nanoplatform loaded with scrambled siRNA (Fig. 4B). It takes a finite amount of time for suppression and DJ-1 protein turnover to initiate an anti-proliferative effect.

We also determined that the combinatorial treatment results in sufficient increase of intracellular ROS level in both cells as compared to PDT alone, suggesting an important role of DJ-1 suppression in ROS elevation (Fig. 4C and D). Following combinatorial treatment, the PY1 assay revealed an increase of H_2O_2 intracellular level (stable form of ROS) by 140% and 85% in ES2 and A2780/AD cells, respectively, as compared to PDT alone. The cell lines treated with either PPI-Pc or combination of both PPI-Pc and PPI-siRNA under dark conditions showed negligible change in the intracellular ROS levels (Fig. 4C and D).

In vivo evaluation of combinatorial ROS-elevating therapy

For animal studies, A2780/AD ovarian cancer cells, which demonstrated a more pronounced response to the combinatorial treatment, were subcutaneously transplanted into the right flank of nude mice. When the tumor volume reached 40 mm^3, PPI-siRNA nanoplatform loaded with *DJ-1* siRNA were administered intravenously 24 h prior to injection of PPI-Pc. After 24 h following a PPI-Pc injection ,corresponding tumors and controls were exposed for 10 min to a single dose of light generated by 690 nm laser diode. Tumors treated with PDT or combinatorial therapies

shrank gradually and were almost eradicated from the mice on the 15th day after the treatment (Fig. 5A, magenta and dark yellow curves). However, tumors treated with PDT only started to regrow on day 16 after commencement of the treatment (Fig. 5A, magenta curve). In contrast, combinatorial therapy showed no evidence of cancer recurrence in the 25 days follow-up period (Fig. 5A, dark yellow curve). Mice treated with (a) saline, (b) 690 nm light only and (c) PPI-Pc under dark conditions grew rapidly with a similar rate (Fig. 5A). Despite the strong anticancer effect, the body weights of the mice increased continuously, indicating that there were no weight loss-causing side effects (Fig. 5B).

DJ-1 siRNA only delivered by the developed nanoplatform inhibited the tumors growth on day 15 after the injection and the tumor volumes (500 mm^3) remained constant throughout the duration of the study (Fig. 5A, olive curve). A similar response was detected after treatment of the mice with both PPI-siRNA and PPI-Pc under dark conditions (Fig. 5A, navy curve). The observed therapeutic effect could be explained by the suppression of the DJ-1 protein causing a decrease in cancer cell proliferation, which is in good agreement with the corresponding *in vitro* studies (Fig. 4B). The DJ-1-directed antibody immunofluorescence staining of the tumor tissues verified that PPI-siRNA was able to deliver *DJ-1* siRNA to the cancer cells and substantially inhibited the targeted protein (Fig. 6, top images).

H&E staining indicated that tumor tissue from the combinatorial treatment group exhibited significantly more damage and loss of stained nuclei when compared to tumors collected from the PDT treated group (Fig. 6 bottom images). In the control groups, negligible damage and loss of stained nuclei were observed. Furthermore, Hoechst staining was used to quantify the number of cells in the various tumor samples that underwent nuclear condensation, and membrane blebbing – the hallmarks of cellular apoptosis.[43] Obtained results indicated that in comparison to

the controls there was a 3.2-and 6.5-fold increase in the number of apoptotic cells in the tumor samples after PDT and combinatorial treatment, respectively (Fig. 7). The increase in the number of apoptotic cells in the tumor tissues after treatment with PPI-siRNA or PPI-siRNA in combination with PPI-Pc under dark conditions was only 1.42 fold. This result strongly indicates that the combinatorial treatment substantially elevates cellular apoptosis.

Discussion

To exploit the potential of both Pc and siRNA as therapeutic agents for novel ROS-induced therapy, we constructed two separate vehicles based on the PPI dendrimers, PPI-siRNA and PPI-Pc, which can transport *DJ-1* siRNA and Pc sequentially to ovarian cancer cells (Fig. 1C and 2).

The selection of a sequential delivery approach for the employed therapeutic agents is warranted by the fact that the half-life of the DJ-1 protein in the cytosol is estimated to be around 24-30 h.[44, 45] Thus, suppression of *DJ-1* mRNA at least 24 h prior to PDT is required to sufficiently decrease the concentration of cytosolic DJ-1 protein and to elicit a therapeutic combinatorial response. In the absence of intracellular DJ-1 protein, ROS levels and apoptosis of cancer cells are hypothesized to be effectively increased via Pc's ROS elevating cytotoxic mechanism of action (Fig. 1C). In addition, it is challenging to achieve the desired concentration ratio of Pc and siRNA in a single nanocarrier to reach the required synergistic effect.

To evaluate *in vitro* efficiency of the developed ROS-induced combinatorial therapy for cancer treatment, two LHRH-positive ovarian cancer cell lines, ES2 and A2780/AD were used. These cell lines are characterized by different basal levels of DJ-1 protein (Fig. 3A) and thus, allowed us to evaluate the effect of the intracellular DJ-1 levels on the efficacy of our combinatorial therapy. ES2 cells, which exhibited lower DJ-1 protein expression, were more

sensitive to PDT (Fig. 3B). These results indicate that higher cellular levels of DJ-1could increase the resistance of cancer cells to ROS-mediated therapy and are a significant cytoprotective factor against exogenous ROS,[19] especially when the latter is present at lower concentrations. These data are in a good agreement with previous reports, which implicated DJ-1 as an intracellular sensor for oxidative stress[19] and postulated its upregulation protects cancer cells against different oxidative agents.[46-51]

Furthermore, we revealed that suppression of DJ-1 protein enhances the therapeutic efficacy of PDT (Fig. 3 C and D) and this enhancement was accompanied by substantial increase of intracellular ROS level as compared to PDT alone in both cancer cell lines (Fig. 4 C and D). It is noteworthy that decrease in cell viability after treatment with the combinatorial approach when compared to PDT alone was more pronounced in A2780/AD cells, which are characterized by higher basal level of DJ-1 protein (Fig. 3D). Higher expression of DJ-1 in A2780/AD cells suggests a more responsive defense system toward ROS, and thus more pronounced improvement in the PDT effect after DJ-1 suppression. These data are in line with previous reports which also revealed that suppression of the DJ-1 protein could lead to a weakened antioxidant defense in cancer cells and enhanced efficacy of ROS-induced agents.[19, 48, 51]

Animal studies further revealed that the ovarian cancer tumors exposed to a single dose of a combinatorial therapy were completely eradicated from the mice and the treated animals showed no evidence of cancer recurrence (Fig. 5A). In contrast, tumors treated with PDT alone started to regrow on day 16 after commencement of the treatment. The initial eradication of cancer tumors after treatment with a single dose of a PDT could be explained by a fact that Pc could generate both ROS and heat under exposure to NIR light.[26] Therefore, Pc-generated hyperthermia can complement a PDT and provide the strong initial response of cancer tumors. Further,

combination of Pc-mediated phototherapy with DJ-1 gene suppression provides a superior therapeutic effect and prevents cancer regrowth.

In summary, the development and evaluation of the novel ROS-induced therapy and the required nanoplatforms for targeted delivery of Pc and siRNA are reported. Efficiency of the delivered *DJ-1* siRNA and Pc to respectively downregulate the targeted gene and generate intracellular ROS in the human ovarian carcinoma cells were validated. Remarkably, siRNA-mediated silencing of *DJ-1* expression substantially enhanced the anticancer activity of PDT and this effect was more pronounced in ovarian carcinoma cells, which are characterized by higher basal levels of DJ-1. Moreover, the enhancement in cell death was accompanied by at least an 85% increase in intracellular ROS levels compared to cells treated with PDT alone. Thus, our data reveal an important role of the *DJ-1* gene as a key player in regulating cellular death mediated by ROS-generating PDT. Furthermore, our study establishes a prospective therapeutic approach against ovarian cancer - the tumors exposed to a single dose of a combinatorial therapy were completely eradicated from the mice. Future studies will address the translational aspects of this approach.

Appendix A. Supplementary Materials

Supplementary materials to this article can be found online.

References

1. 2015. Cancer facts and figures, American Cancer Society. http://www.cancer.org/research/cancerfactsstatistics/cancerfactsfigures2014/

2. Lim MC, Seo SS, Kang S, Kim SK, Kim SH, Yoo CW, et al. Intraoperative image-guided surgery for ovarian cancer. *Quant Imaging Med Surg* 2012;**2**:114-7.

3. van Dam GM, Themelis G, Crane LM, Harlaar NJ, Pleijhuis RG, Kelder W, et al. Intraoperative tumor-specific fluorescence imaging in ovarian cancer by folate receptor-alpha targeting: first in-human results. *Nat Med* 2011;**17**:1315-9.

4. Bristow RE, Tomacruz RS, Armstrong DK, Trimble EL, Montz FJ. Survival effect of maximal cytoreductive surgery for advanced ovarian carcinoma during the platinum era: a meta-analysis. *J Clin Oncol* 2002;**20**:1248-59.

5. Lim MC, Kang S, Lee KS, Han SS, Park SJ, Seo SS, et al. The clinical significance of hepatic parenchymal metastasis in patients with primary epithelial ovarian cancer. *Gynecol Oncol* 2009;**112**:28-34.

6. Dowdy SC, Mariani A, Cliby WA, Haddock MG, Petersen IA, Sim FH, et al. Radical pelvic resection and intraoperative radiation therapy for recurrent endometrial cancer: technique and analysis of outcomes. *Gynecol Oncol* 2006;**101**:280-6.

7. Elias D, Goere D, Dumont F, Honore C, Dartigues P, Stoclin A, et al. Role of hyperthermic intraoperative peritoneal chemotherapy in the management of peritoneal metastases. *Eur J Cancer* 2014;**50**:332-40.

8. Yap OW, Kapp DS, Teng NN, Husain A. Intraoperative radiation therapy in recurrent ovarian cancer. *Int J Radiat Oncol Biol Phys* 2005;**63**:1114-21.

9. Agostinis P, Berg K, Cengel KA, Foster TH, Girotti AW, Gollnick SO, et al. Photodynamic therapy of cancer: an update. *CA Cancer J Clin* 2011;**61**:250-81.

10. Dolmans DE, Fukumura D, Jain RK. Photodynamic therapy for cancer. *Nature Rev Cancer* 2003;**3**:380-7.

11. Gorrini C, Harris IS, Mak TW. Modulation of oxidative stress as an anticancer strategy. *Nature Rev Drug Discovery* 2013;**12**:931-47.

12. Hileman EO, Liu J, Albitar M, Keating MJ, Huang P. Intrinsic oxidative stress in cancer cells: a biochemical basis for therapeutic selectivity. *Cancer Chemother Pharmacol* 2004;**53**:209-19.

13. Das TP, Suman S,Damodaran C. Induction of reactive oxygen species generation inhibits epithelial-mesenchymal transition and promotes growth arrest in prostate cancer cells. *Mol Carcinog* 2014;53:537-47.

14. Friedberg JS. Photodynamic therapy for malignant pleural mesothelioma: the future of treatment? *Expert Rev Respir Med* 2011;**5**:49-63.

15. Rigual NR, Shafirstein G, Frustino J, Seshadri M, Cooper M, Wilding G, et al. Adjuvant intraoperative photodynamic therapy in head and neck cancer. *JAMA Otolaryngol Head Neck Surg* 2013;**139**:706-11.

16. Zilidis G, Aziz F, Telara S, Eljamel MS. Fluorescence image-guided surgery and repetitive Photodynamic Therapy in brain metastatic malignant melanoma. *Photodiagn Photodyn Ther* 2008;**5**:264-6.

17. Casas A, Di Venosa G, Hasan T, Al B. Mechanisms of resistance to photodynamic therapy. *Curr Med Chem* 2011;**18**:2486-515.

18. Agnani D, Camacho-Vanegas O, Camacho C, Lele S, Odunsi K, Cohen S, et al. Decreased levels of serum glutathione peroxidase 3 are associated with papillary serous ovarian cancer and disease progression. *J Ovarian Res* 2011;**4**:18.

19. Cao J, Lou S, Ying M, Yang B. DJ-1 as a human oncogene and potential therapeutic target. *Biochem Pharmacol* 2015;**93**:241-50.

20. Hu Y, Rosen DG, Zhou Y, Feng L, Yang G, Liu J, et al. Mitochondrial manganese-superoxide dismutase expression in ovarian cancer: role in cell proliferation and response to oxidative stress. *J Biol Chem* 2005;**280**:39485-92.

21. Shim GS, Manandhar S, Shin DH, Kim TH, Kwak MK. Acquisition of doxorubicin resistance in ovarian carcinoma cells accompanies activation of the NRF2 pathway. *Free Radic Biol Med* 2009;**47**:1619-31.

22. Clements CM, McNally RS, Conti BJ, Mak TW, Ting JPY. DJ-1, a cancer- and Parkinson's disease-associated protein, stabilizes the antioxidant transcriptional master regulator Nrf2. *Proc Natl Acad Sci U S A* 2006;**103**:15091-15096.

23. Hod Y. Differential control of apoptogis by DJ-1 in prostate benign and cancer cells. *J Cell Biochem* 2004;**92**:1221-1233.

24. Fan J, Ren HG, Jia NL, Fei E, Zhou T, Jiang P, et al. DJ-1 decreases Bax expression through repressing p53 transcriptional activity. *J Biol Chem* 2008;**283**:4022-4030.

25. Sekkat N, van den Bergh H, Nyokong T, Lange N. Like a Bolt from the Blue: Phthalocyanines in Biomedical Optics. *Molecules* 2012;**17**:98-144.

26. Taratula O, Patel M, Schumann C, Naleway MA, Pang AJ, He H. Phthalocyanine-loaded graphene nanoplatform for imaging-guided combinatorial phototherapy. *Int J Nanomed* 2015;**10**:2347-62.

27. Taratula O, Schumann C, Naleway MA, Pang AJ, Chon KJ. A multifunctional theranostic platform based on phthalocyanine-loaded dendrimer for image-guided drug delivery and photodynamic therapy. *Mol Pharm* 2013;**10**:3946-58.

28. Huang C, Li M, Chen C, Yao Q. Small interfering RNA therapy in cancer: mechanism, potential targets, and clinical applications. *Expert Opin Ther Targets* 2008;**12**:637-45.

29. Seth S, Johns R, Templin MV. Delivery and biodistribution of siRNA for cancer therapy: challenges and future prospects. *Ther Deliv* 2012;**3**:245-261.

30. Taratula O, Schumann C, Duong T, Taylor KL, Taratula O. Dendrimer-encapsulated naphthalocyanine as a single agent-based theranostic nanoplatform for near-infrared fluorescence imaging and combinatorial anticancer phototherapy. *Nanoscale* 2015;**7**:3888-902.

31. Dani RK, Schumann C, Taratula O. Temperature-tunable iron oxide nanoparticles for remote-controlled drug release. *AAPS PharmSciTech* 2014;**15**:963-72.

32. Shah V, Taratula O, Garbuzenko OB, Taratula OR, Rodriguez-Rodriguez L, Minko T. Targeted nanomedicine for suppression of CD44 and simultaneous cell death induction in ovarian cancer: an optimal delivery of siRNA and anticancer drug. *Clin Cancer Res* 2013;**19**:6193-204.

33. Dickinson BC, Huynh C, Chang CJ. A palette of fluorescent probes with varying emission colors for imaging hydrogen peroxide signaling in living cells. *J Am Chem Soc* 2010;**132**:5906-15.

34. Mishra GP, Nguyen D, Alani AW. Inhibitory effect of paclitaxel and rapamycin individual and dual drug-loaded polymeric micelles in the angiogenic cascade. *Mol Pharm* 2013;**10**:2071-8.

35. Taratula OR, Patel M, Schumann C, Naleway MA, Pang AJ, He H, et al. Phthalocyanine-loaded graphene nanoplatform for imaging-guided combinatorial phototherapy. *Int J Nanomed* 2015;**10**:2347-2362.

36. Taratula O, Garbuzenko OB, Kirkpatrick P, Pandya I, Savla R, Pozharov VP, et al. Surface-engineered targeted PPI dendrimer for efficient intracellular and intratumoral siRNA delivery. *J Control Release* 2009;**140**:284-293.

37. Taratula O, Savla R, He H, Minko T. Poly (propyleneimine) dendrimers as potential siRNA delivery nanocarrier: from structure to function. *Int J Nanotechnol* 2011;**8**:35-62.

38. Shah V, Taratula O, Garbuzenko OB, Taratula OR, Rodriguez-Rodriguez L, Minko T. Targeted nanomedicine for suppression of CD44 and simultaneous cell death induction in ovarian cancer: an optimal delivery of siRNA and anticancer drug. *Clin Cancer Res* 2013;**19**:6193-6204.

39. Alexis F, Pridgen E, Molnar LK, Farokhzad OC. Factors affecting the clearance and biodistribution of polymeric nanoparticles. *Mol Pharm* 2008;**5**:505-515.

40. Kojima C, Toi Y, Harada A, Kono K. Preparation of poly(ethylene glycol)-attached dendrimers encapsulating photosensitizers for application to photodynamic therapy. *Bioconjug Chem* 2007;**18**:663-70.

41. Arencibia JM, Bajo AM, Schally AV, Krupa M, Chatzistamou I, Nagy A. Effective treatment of experimental ES-2 human ovarian cancers with a cytotoxic analog of luteinizing hormone-releasing hormone AN-207. *Anticancer Drugs* 2002;**13**:949-56.

42. Volker P, Grundker C, Schmidt O, Schulz KD, Emons G. Expression of receptors for luteinizing hormone-releasing hormone in human ovarian and endometrial cancers: frequency,

autoregulation, and correlation with direct antiproliferative activity of luteinizing hormone-releasing hormone analogues. *Am J Obstetr Gynecol* 2002;**186**:171-9.

43. Fazal N, Al-Ghoul WM. Thermal injury-plus-sepsis contributes to a substantial deletion of intestinal mesenteric lymph node CD4 T cell via apoptosis. *Int J Biol Sci* 2007;**3**:393-401.

44. Gan L, Johnson DA, Johnson JA. Keap1-Nrf2 activation in the presence and absence of DJ-1. *Eur J Neurosci* 2010;**31**:967-77.

45. Honbou K, Suzuki NN, Horiuchi M, Niki T, Taira T, Ariga H, et al. The crystal structure of DJ-1, a protein related to male fertility and Parkinson's disease. *J Biol Chem* 2003;**278**:31380-4.

46. Inberg A, Linial M. Protection of pancreatic beta-cells from various stress conditions is mediated by DJ-1. *J Biol Chem* 2010;**285**:25686-98.

47. Ismail IA, Shakor AB, Hong SH. DJ-1 protects breast cancer cells against 2'-benzoyloxycinnamaldehyde-induced oxidative stress independent of Nrf2. *J Cell Physiol* 2015

48. Liu H, Wang M, Li M, Wang D, Rao Q, Wang Y, et al. Expression and role of DJ-1 in leukemia. *Biochem Biophys Res Commun* 2008;**375**:477-83.

49. MacKeigan JP, Clements CM, Lich JD, Pope RM, Hod Y,Ting JP. Proteomic profiling drug-induced apoptosis in non-small cell lung carcinoma: identification of RS/DJ-1 and RhoGDIalpha. *Cancer Res* 2003;**63**:6928-34.

50. Raninga PV, Trapani GD,Tonissen KF. Cross Talk between Two Antioxidant Systems, Thioredoxin and DJ-1: Consequences for Cancer. *Oncoscience* 2014;**1**:95-110.

51. Zhu H, Liao SD, Shi JJ, Chang LL, Tong YG, Cao J, et al. DJ-1 mediates the resistance of cancer cells to dihydroartemisinin through reactive oxygen species removal. *Free Radic Biol Med* 2014;**71**:121-32.

Figures Legends:

Figure 1. Preparation of the PPI dendrimer-based nanoplatforms for targeted delivery of **(A)** Pc (PPI-Pc) and **(B)** *DJ-1* siRNA (PPI-siRNA). **(C)** Schematic illustration of the ROS-induced combinatorial therapy for cancer treatment. **Step 1:** The siRNA molecules delivered by PPI-siRNA via LHRH-receptor mediated endocytosis to cancer cells suppress the targeted *DJ-1* gene and inhibit the intracellular ROS defense system. **Step 2:** The sequentially delivered Pc molecules by PPI-Pc generate intracellular ROS after activation with NIR light. Combining a boost in the intracellular ROS level with inhibition of the cellular ROS defense system results in efficient apoptosis of cancer cells.

Figure 2. Flow cytometry analysis of cellular internalization of **(A)** PPI-Pc and **(B)** PPI-siRNA after incubation with ES2 ovarian carcinoma cells for 24 h. **(C)** Expression of *DJ-1* mRNA in ES2 cells after treatment with media and PPI-siRNA for 24 h. **(Inset)** Representative Western blot images of DJ-1 and β-actin expression in ES2 cells after treatment with media and PPI-siRNA for 24 h. **(D)** Relative singlet oxygen level in ES2 cells treated with PPI-Pc at the following concentrations: 0, 32, 63 and 125 ng/mL for 24 h and irradiated for 5 min using 690 nm laser diode (0.3 W/cm^2). PPI-Pc transfected cells treated under dark conditions and cells incubated with media were used as the controls. Means ± SD are shown. *P < 0.005 when compared with cells incubated with fresh media.

Figure 3. (A) Relative basal level of *DJ-1* mRNA in A2780/AD and ES2 ovarian cancer cells as compared to non-malignant HUVEC cells. The expression of *DJ-1* in HUVEC cells was set as 1.

Means ± SD are shown. *P < 0.05 and **P < 0.005 when compared with HUVEC cells. **Inset:** Western blot images of DJ-1 protein expression in HUVEC, A2780/AD and ES2 cells. β-Actin was used as the endogenous control. **(B)** Viability of ES2 and A2780/AD cells treated with PDT only at various Pc concentrations. Controls represent viability of non-treated cells (Pc = 0 ng/mL) irradiated with a 690 nm laser diode (0.3 W/cm^2) for 5 min. *P < 0.05 and **P < 0.005 when compared with PDT treated A2780/AD cells. Viability of ES2 (**C**) and A2780/AD (**D**) cells treated with PDT only and combinatorial therapy (*DJ-1* siRNA + PDT) at various Pc concentrations. Controls represent viability of non-treated cells (Pc = 0 ng/mL, red bars) and the cells treated with PPI-siRNA only (siRNA=1 μM, white bars) after exposure to a laser diode (690 nm, 0.3 W/cm^2) for 5 min. *P < 0.05 and **P < 0.005 when compared with PDT treated cells. **Inset:** Western blot images of DJ-1 protein expression in A2780/AD and ES2 cells after treatment with PPI-siRNA for 24 h.

Figure 4. (A) Viability of ES2 and A2780/AD cells treated with PPI-siRNA (*DJ-1* siRNA = 1 μM) for 48 h under dark and light (690 nm, 0.3 W/cm^2) conditions. **(B)** Real-time proliferation profiles of A2780/AD cells after treatment with fresh media (control) and PPI-based nanoplatforms loaded with either scrambled or *DJ-1*-targeted siRNA molecules (siRNA = 1 μM). Relative level of hydrogen peroxide (H_2O_2) in ES2 **(C)** and A2780/AD cells **(D)** after treatment with PDT (Pc = 63 ng/mL, 0.3 W/cm^2) and combinatorial therapy (siRNA = 1 μM, Pc = 63 ng/mL, 0.3 W/cm^2). Cells transfected with the appropriate nanoplatforms and treated under dark conditions and cells incubated with media were used as the controls. Means ± SD are shown. *P < 0.05 and **P < 0.005 when compared with cells treated under dark conditions.

Figure 5. Changes in tumor volumes **(A)** and body weights of mice **(B)** after the following treatments: (1) saline (control), (2) tumor irradiation with 690 nm light (Light), (3) PPI-Pc (Pc dark), (4) PPI-siRNA (DJ-1), (5) PPI-Pc in combination with 690 nm light (PDT), (6) PPI-siRNA in combination with PPI-Pc (DJ-1/Pc dark) and (7) PPI-siRNA in combination with PPI-Pc followed by 690 nm light irradiation (DJ-1/PDT). Means ± SD are shown.

Figure 6. Expression of DJ-1 protein (immunohistochemistry) in tumor tissues (top images) and H&E stained tumor sections after treatment with the indicated formulations.

Figure 7. Percent of apoptotic cells in tumor tissues after treatment with the indicated formulations. The number of apoptotic cells was determined in tumor tissues stained with Hoechst. Means ± SD are shown. $*P < 0.05$ when compared with control.

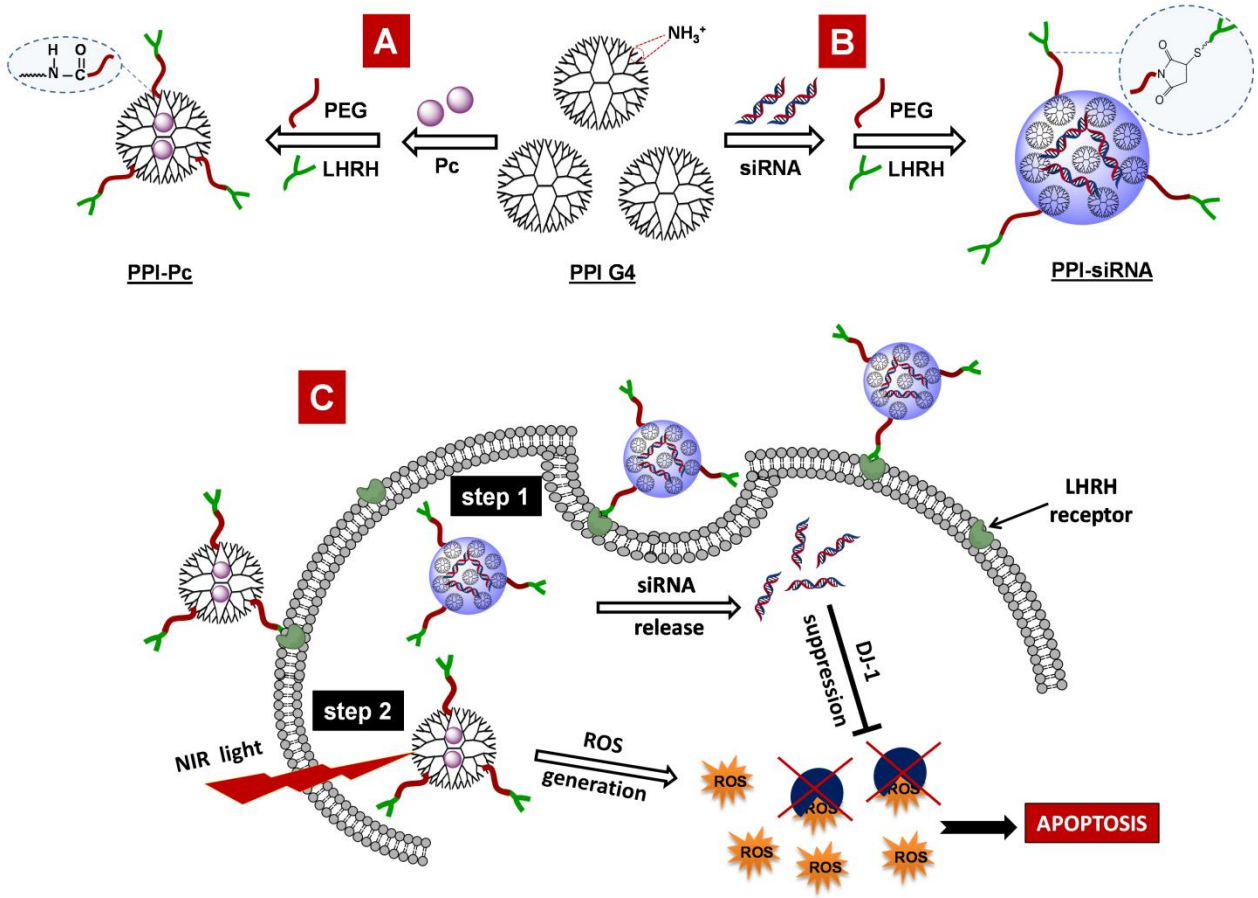

Figure 1

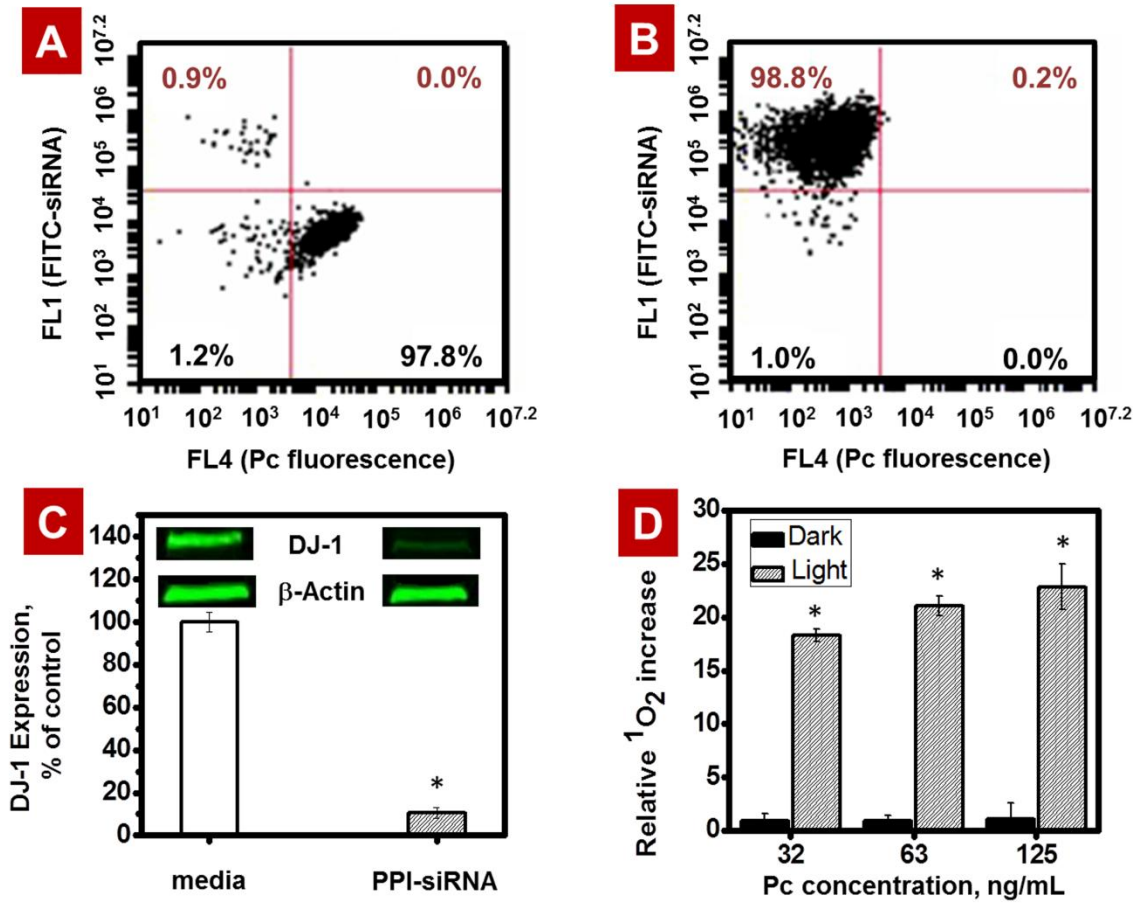

Figure 2

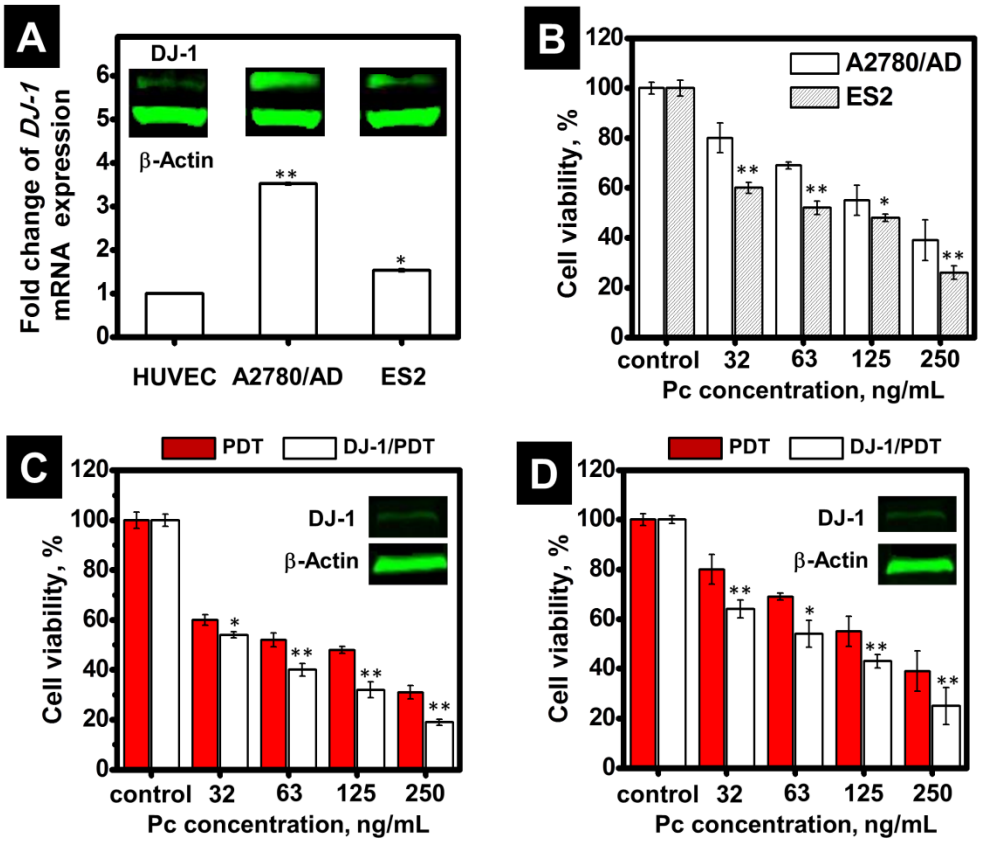

Figure 3

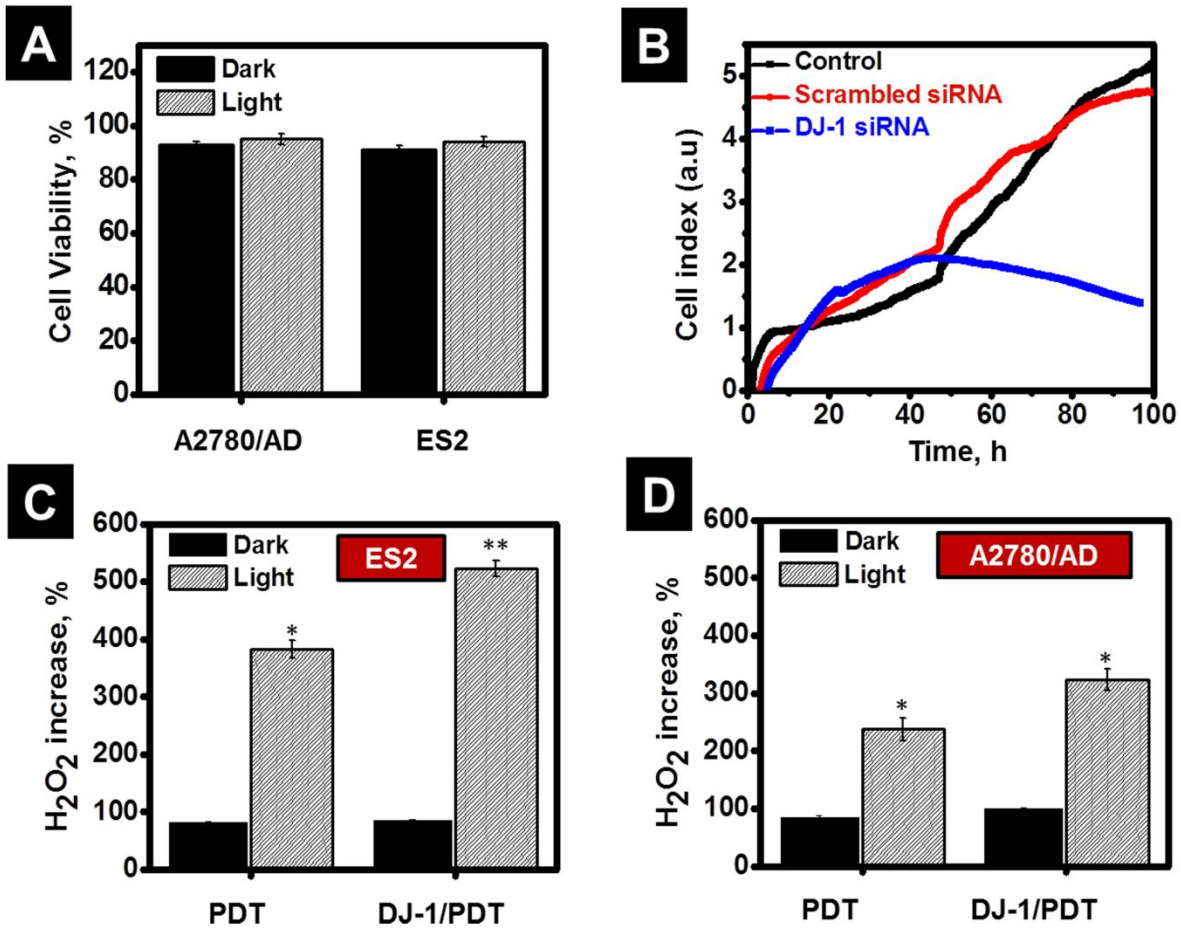

Figure 4

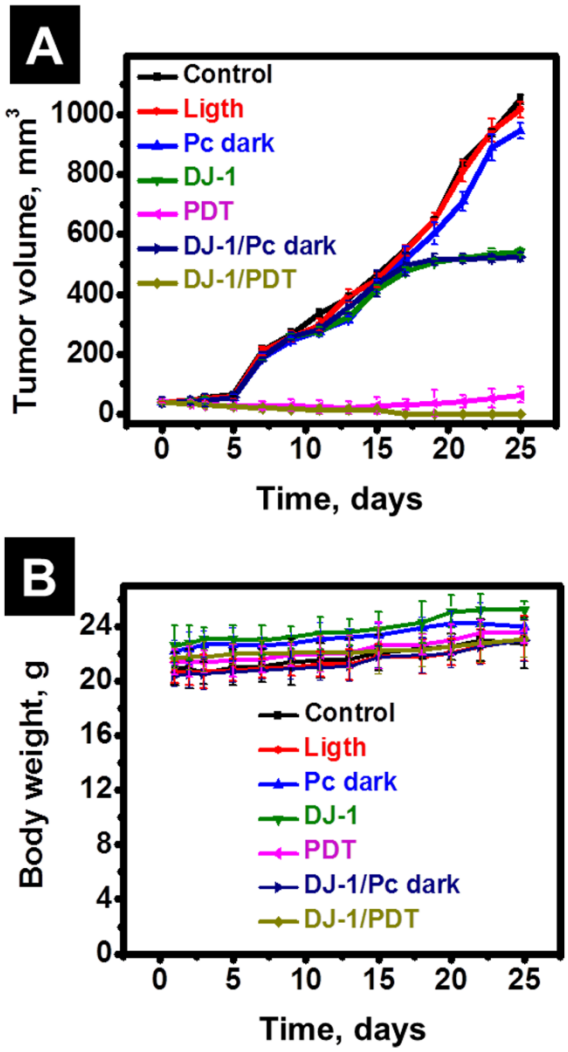

Figure 5

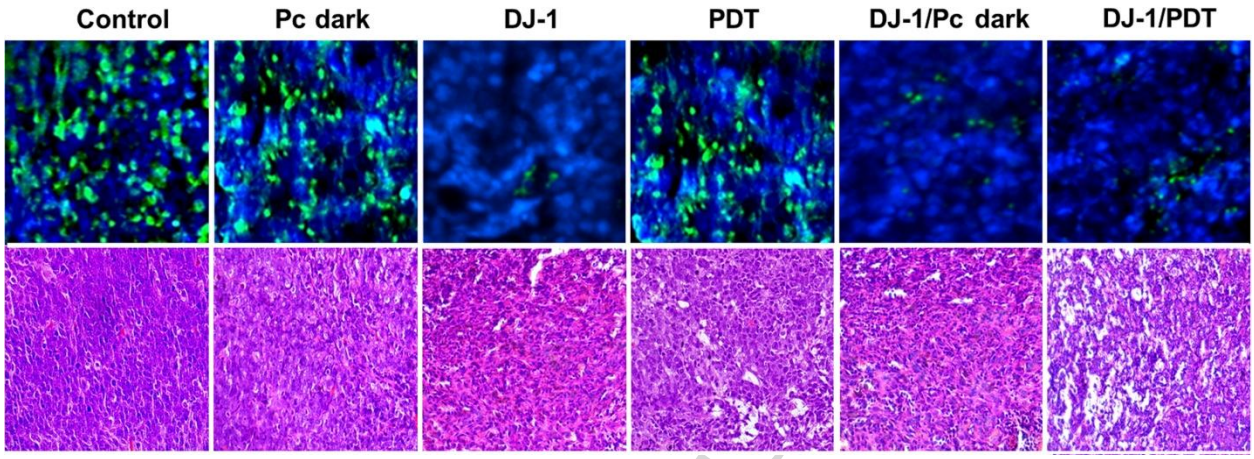

Figure 6

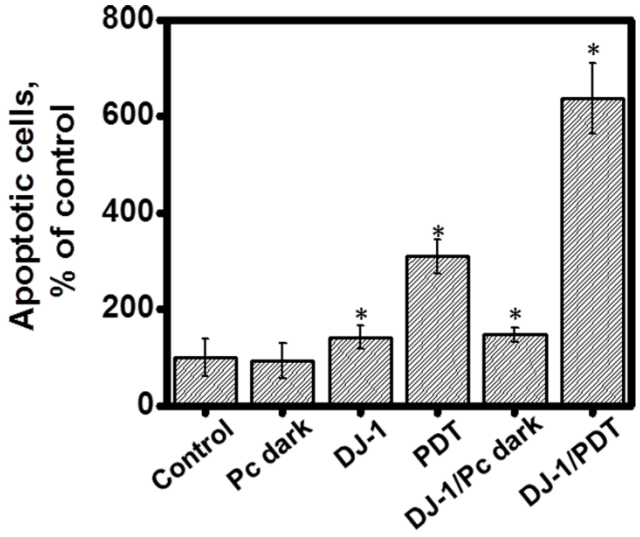

Figure 7

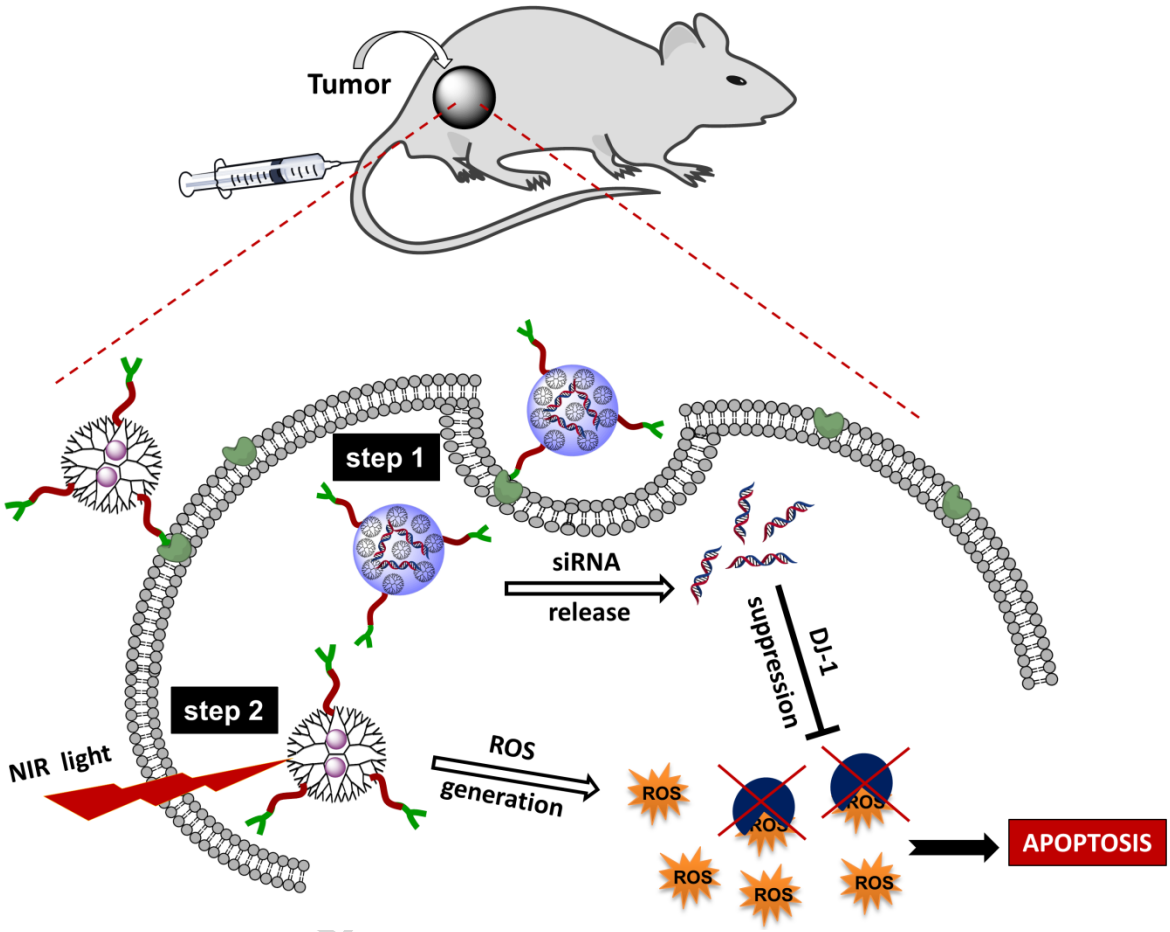

Graphical Abstract

We have developed a novel ROS-induced therapy for intraoperative ovarian cancer treatment using the combinatorial effect of cancer-targeted photodynamic therapy associated with the suppression of the intracellular ROS defense system. The constructed cancer-targeted nanomedicine platforms are capable of sequential delivery of *DJ-1* siRNA and photosensitizer (Ps) to the cancer tumors. The delivered siRNA suppresses the targeted *DJ-1* gene and inhibits the intracellular ROS defense mechanism. The sequentially delivered Ps molecules generate intracellular ROS after activation with NIR light. Combining a boost in the intracellular ROS levels with attenuation of the cellular tolerance toward ROS results in an increase of apoptotic cancer cells.